

On the Performance of Using Multiple Transmit and Receive Antennas in Pulse-Based Ultrawideband Systems

Li-Chun Wang, *Member, IEEE*, Wei-Cheng Liu, *Student Member, IEEE*, and Kuan-Jiin Shieh

Abstract—This paper presents an analytical expression for the signal-to-noise ratio (SNR) of the pulse position modulated (PPM) signal in an ultrawideband (UWB) channel with multiple transmit and receive antennas. A generalized fading channel model that can capture the cluster property and the highly dense multipath effect of the UWB channel is considered. Through simulations, it is demonstrated that the derived analytical model can accurately estimate the mean and variance properties of the pulse-based UWB signals in a frequency-selective fading channel. Furthermore, the authors investigate to what extent the performance of the PPM-based UWB system can be further enhanced by exploiting the advantage of multiple transmit antennas or receive antennas. Numerical results show that using multiple transmit antennas in the UWB channel can improve the system performance in the manner of reducing signal variations. However, because of already possessing rich diversity inherently in the UWB channel, using multiple transmit antennas does not provide diversity gain in the strict sense [i.e., improving the slope of bit error rate (BER) versus SNR] but can possibly reduce the required fingers of the RAKE receiver for the UWB channel. Furthermore, because multiple receive antennas can provide higher antenna array combining gain, the multiple receive antennas technique can be used to improve the coverage performance for the UWB system, which is crucial for a UWB system due to the low transmission power operation.

Index Terms—Pulse position modulation (PPM), time-switched transmit diversity (TSTD), ultrawideband (UWB).

I. INTRODUCTION

WIRELESS systems continue to pursue even higher data rates and better quality. The ultrawideband (UWB) technique and space-time processing techniques are two promising techniques to achieve this objective. However, how to merge these two techniques together to further increase the data rates is not an easy task. This paper investigates how multiple transmit/receive antennas and the UWB system can function together to exploit the synergy of marrying these two advanced techniques.

Manuscript received July 10, 2003; revised April 5, 2004; accepted October 10, 2004. The editor coordinating the review of this paper and approving it for publication is A. Svensson. This work was supported jointly by the National Science Council and the Program of Promoting University Excellence of Ministry of Education, Taiwan, under Contract NSC93-2213-E-009-097 and Contract EX-91-E-FA06-4-4.

The authors are with the Department of Communication Engineering, National Chiao-Tung University, Hsinchu 300, Taiwan (e-mail: lichun@cc.nctu.edu.tw).

Digital Object Identifier 10.1109/TWC.2005.858009

In general, the UWB system can be classified into three kinds, namely 1) the multiband orthogonal frequency division multiplexing approach; 2) the time-hopping ultrawideband (TH-UWB) system; and 3) the direct-sequence ultrawideband (DS-UWB) [1]. In this paper, we focus on the TH-UWB system with pulse position modulation (PPM). Through modulating an information bit over extremely large bandwidth of several gigahertz, the TH-UWB system can possess many nice properties, including the following: high path resolution in the dense multipath fading environment [2]–[4]; smooth noise-like frequency-domain characteristics [2]; carrierless transmission [3]; and low transmission power operation [2], [3], [5].

Besides UWB, space-time processing transmit diversity techniques, such as space-time block code (STBC) or space-time trellis code (STTC), is another important research area recently [6]–[9]. It is noteworthy that these space-time processing transmit diversity schemes are originally designed for signals with information bits modulated by the amplitude or phase of a signal, rather than the occurrence time of a signal. Since a PPM signal represents its data information bit according to the pulse displacement from a specified time reference. Thus, directly applying STTC or STBC in the PPM-based UWB system may not be easy, especially in a highly dense frequency-selective fading channel [10].

In spite of numerous advantages for the UWB system, it is crucial to make the best use of the radiation power because of its extremely low transmitted power. Consequently, although fading may not be serious in the pulsed mode UWB system, receive antenna diversity is suggested for the UWB system to improve energy capture [11], [12]. In the literature, fewer papers have been reported to address the issue of employing transmit diversity for the pulsed UWB system, except [13] and [14]. In [13], Weisenhorn and Hirt evaluated the performance of the pulse-amplitude modulation (PAM) signals in the UWB multiple-input multiple-output (MIMO) channel. In [14], Yang and Giannakis proposed an STBC scheme for the PPM-based UWB system in the flat fading real channel, where the received pulses through the radio channel are assumed to be orthogonal with each other.

To the best of our knowledge, it has not been seen that the PPM-based UWB are evaluated using multiple transmit and receive antennas in a frequency-selective multipath fading environment. The objective of this paper is to investigate to what extent can transmit/receive diversity further improve the performance for the PPM-based UWB system.

Toward this end, we first analyze the statistical properties of the PPM signals in a generalized frequency-selective fading model proposed for the UWB system [15]. To accurately evaluate the UWB system performance, choosing an appropriate channel model is very crucial. In the literature, many models have been reported to characterize the UWB channel, such as [5] and [16]–[21]. In particular, according to the measurement results of [16] and [19], Zhu *et al.* [15] proposed a generalized fading channel model for the UWB application, which can possess two major properties of the UWB channel, namely: 1) clustering property and 2) highly frequency-selective fading. Through simulations, we demonstrate that the derived analytical model can accurately estimate the first-order and the second-order statistics of the pulse-based UWB signals in the considered UWB channel model.

Second, we investigate the effect of applying the transmit/receive antenna diversity techniques in the UWB system. Specifically, we consider a time-switched transmit diversity (TSTD) scheme [22] at the transmitter end, and the template-based pulse detection using antenna diversity at the receiver end [12]. Through simulations, we show that using multiple transmit antennas in the UWB channel can improve the system performance in the manner of reducing signal variations. Because of already possessing rich diversity inherently, using multiple transmit antennas does not provide diversity gain in the strict sense [i.e., the slope of bit error rate (BER) versus signal-to-noise ratio (SNR)], but can reduce the complexity of the RAKE receiver. As for the effect of receive diversity, we demonstrate that the multiple receive antennas can improve the performance of the UWB system by providing higher antenna array combining gain even without providing the diversity gain in the strict sense.

The rest of the paper is organized as follows. Section II describes a generalized frequency-selective fading model for the UWB system. In Section III, we discuss the signal model and the template-based detection scheme for PPM signals. In Section IV, we derive the closed-form expression for the mean and variance of the PPM signal subject to the impact of the considered UWB channel. In Section V, we discuss the effect of applying the multiple transmit and receive antennas technique in UWB systems. In Section VI, we present the analytical and simulation results. We give our conclusions in Section VII.

II. CHANNEL MODEL

To evaluate the performance of a UWB system with multipath fading, the discrete impulse response of the channel is considered, which is given as

$$h(t) = \sum_{l=0}^{L_c-1} \xi_l \Delta(t - lT_c) \quad (1)$$

where L_c is the number of resolvable multipath components, T_c is the chip duration or the length of the time bin, and $\Delta(t)$ is the Dirac delta function. In (1), the amplitude fading factor on path l (denoted as ξ_l) can be expressed as

$$\xi_l = b_l a_l \quad (2)$$

where b_l is equiprobable to take on the value ± 1 and a_l is the Nakagami fading term. The term b_l is used to account for the random pulse inversion that can occur due to reflections, as observed in the measurements [21].

In this paper, we consider a UWB channel characterized by the following three major properties [15]:

- 1) Gamma distribution to describe each resolvable path power;
- 2) a modified Poisson process to characterize the clustering property of the UWB channel and the number of the simultaneous arrival paths;
- 3) exponential decay to model the average resolvable path power in the time domain.

A. PDF of the Received Signal Power

For the l th path with path gain ξ_l and n_l simultaneous arrival paths, the probability density function (PDF) of the received signal power $y = \xi_l^2 = a_l^2$ can be characterized by a Gamma distributed random variable as [19]

$$f_Y(y) = \frac{1}{\sigma_l^{n_l} 2^{\frac{n_l}{2}} \Gamma(\frac{1}{2}n_l)} y^{\frac{n_l}{2}-1} e^{-\frac{y}{2\sigma_l^2}} \quad (3)$$

where $\Gamma(\alpha) = \int_0^\infty t^{\alpha-1} \exp(-t) dt$ and $\sigma_l^2 = (1/n_l)E[a_l^2]$. In the following, we discuss the way to calculate the terms n_l and $E[a_l^2]$.

B. Number of Simultaneous Arrival Paths

The clustering property in the UWB channel can be characterized by a modified Poisson process driven through a two-state Markov chain [16]. If a resolvable path appears in the previous time bin, a Poisson arrival process will be in the high state with μ_H average simultaneous arrival paths; otherwise, it will be in the low state with μ_L average simultaneous arrival paths, where $\mu_H > \mu_L$. Let n_l denote the simultaneous arrival paths in the l th time bin. Then

$$\text{Prob}[n_l = k] = \begin{cases} \frac{\mu_H^k}{k!} e^{-\mu_H}, & \text{when } n_{l-1} \neq 0 \\ \frac{\mu_L^k}{k!} e^{-\mu_L}, & \text{when } n_{l-1} = 0. \end{cases} \quad (4)$$

Note that the transition probability of a Poisson process with a mean of μ_H changing to that with a mean of μ_L can be calculated by $\alpha = e^{-\mu_H}$; or similarly, $\beta = 1 - e^{-\mu_L}$ represents the transition probability from the low state to the high state.

C. Average Resolvable Path Power

We apply the exponential decay model to characterize the received signal power a_l^2 in the time domain [19]. Obviously, if $n_l = 0$, $E[a_l] = 0$. When $n_l \neq 0$

$$E[a_l^2] = \begin{cases} 1, & \text{when } l = 1 \\ \gamma e^{-\eta(l-2)}, & \text{when } l \geq 2 \end{cases} \quad (5)$$

where η is the decay constant and γ is the power adjustment factor except the first path.

III. SIGNAL MODEL AND DETECTION SCHEME

A. Signal Model

Consider a single user employing binary PPM in the UWB channel. Let T_f and T_c be the frame time and the chip time of the PPM signal, respectively. With the transmitted pulse waveform $w_{tr}(t)$, the transmitted signal for the i th message bit $d^{(i)}$ is written as [3]

$$s_{tr}^{(i)} = \sum_{j=0}^{N_p-1} w_{tr} \left(t - jT_f - c_j^{(i)}T_c - d^{(i)}\delta T_c \right) \quad (6)$$

where N_p is the repetition number for one information bit, $\{c_j^{(i)}\}$ is a time-hopping sequence, and δ is the modulation index associated with the message bit, which is normalized to the chip time T_c . The frame time T_f is assumed to be much larger than T_c . In this paper, we assume that the transmitted pulse waveform $w_{tr}(t)$ is

$$w_{tr}(t) = \begin{cases} 1, & 0 \leq t < T_c \\ 0, & \text{otherwise} \end{cases}.$$

With the channel response $h(t)$ and the noise $n(t)$, the received PPM data for the i th information bit is written as

$$s_{rec}^{(i)}(t) = s_{tr}^{(i)} * h(t) + n(t) \\ = \sum_{j=0}^{N_p-1} x \left(t - jT_f - c_j^{(i)}T_c - d^{(i)}\delta T_c \right) + n(t) \quad (7)$$

where the received pulse waveform $x(t) = w_{tr}(t) * h(t)$. Since the goal of this work is focused on the impact of the UWB channel on the PPM signal detection in the single user case, we ignore the time-hopping code. With respect to a particular information bit sampled at the l th time bin within a frame, the desired signal part in (7) can be written as

$$x_l = \sum_{k=0}^{L_c-1} \sum_{j=0}^{N_p-1} \xi_l w_{tr} \left((l-k)T_c - jT_f - d^{(i)}\delta T_c \right) \quad (8)$$

where ξ_l and w_{tr} are defined in (1) and (6).

For the message bit $d^{(i)} = 0$ in the channel response with a length of L_c , the received data \mathbf{r}_0 can be expressed as

$$\mathbf{r}_0 = \mathbf{x}_0 + \mathbf{n} \quad (9)$$

where $\mathbf{x}_0 = [x_1, x_2, \dots, x_{L_c}, \overbrace{0 \dots 0}^{\delta' s 0}]^T$ and $\mathbf{n} = [n_1, n_2, \dots, n_{L_c}, n_{L_c+1}, \dots, n_{L_c+\delta}]^T$. Similarly, for the message bit $d^{(i)} = 1$

$$\mathbf{r}_1 = \mathbf{x}_1 + \mathbf{n} \quad (10)$$

where $\mathbf{x}_1 = [\overbrace{0 \dots 0}^{\delta' s 0}, x_1, x_2, \dots, x_{L_c}]^T$.

B. Signal Detection

Similar to [3], [12], and [23], we consider a template-based detection scheme for the PPM signals. Having two possible output waveforms \mathbf{x}_0 and \mathbf{x}_1 for message bit $d^{(i)} = 0$ and $d^{(i)} = 1$ defined in (9) and (10), respectively, we can choose $\mathbf{p}_0 = \mathbf{x}_0$ and $\mathbf{p}_1 = \mathbf{x}_1$ and represent a template signal \mathbf{p} for the binary PPM case as

$$\mathbf{p} = -\mathbf{p}_0 + \mathbf{p}_1. \quad (11)$$

Now, we take \mathbf{r}_1 as an example. Consider a RAKE receiver with L fingers and denote the processed data z_{p1} as the inner product of the received data \mathbf{r}_1 of (10) and the template \mathbf{p} of (11). Then, we have

$$z_{p1} = \mathbf{p}^T \mathbf{r}_1 = (-\mathbf{p}_0^T + \mathbf{p}_1^T) \mathbf{r}_1 \\ = \sum_{i=1}^L x_i x_i - \sum_{i=1}^{L-\delta} x_i x_{i+\delta} + \sum_{i=1}^L n_{i+\delta} x_i - \sum_{i=1}^L n_i x_i \\ = s_{p1} + r_{p1} + n_{p1} + n_{p0} \quad (12)$$

where $s_{p1} = \sum_{i=1}^L x_i x_i$ is the signal part, $r_{p1} = -\sum_{i=1}^{L-\delta} x_i x_{i+\delta}$ is the redundancy part, $n_{p1} = \sum_{i=1}^L n_{i+\delta} x_i$ is the noise part of the processed data z_{p1} from \mathbf{p}_1 , and $n_{p0} = -\sum_{i=1}^L n_i x_i$ is the noise part of the processed data z_{p1} from \mathbf{p}_0 . From (12), we can use the sum of the pulse correlator outputs as the test statistics to detect the transmitted symbol. Specifically, if the processed data z_{p1} is larger than zero, the transmitted message bit $d^{(i)} = 0$; otherwise, we take the transmitted message bit $d^{(i)} = 1$.

IV. ANALYSIS OF PPM UWB SIGNALS

A. State Probabilities of the Modified Poisson Process

Consider a two-state Markov chain of (4) with the probability $\alpha = e^{-\mu_H}$ changing from the high state to the low state, and the probability $\beta = 1 - e^{-\mu_L}$ changing from the low state to the high state. Then, the transition probability matrix \mathbf{P} is represented as

$$\mathbf{P} = \begin{bmatrix} 1 - \alpha & \alpha \\ \beta & 1 - \beta \end{bmatrix}. \quad (13)$$

According to [24], the i -step transition probability matrix \mathbf{P}^i can be expressed as

$$\mathbf{P}^i = \frac{1}{\alpha + \beta} \begin{bmatrix} \beta & \alpha \\ \beta & \alpha \end{bmatrix} + \frac{(1 - \alpha - \beta)^i}{\alpha + \beta} \begin{bmatrix} \alpha & -\alpha \\ -\beta & \beta \end{bmatrix}. \quad (14)$$

Denote $\pi_H(l)$ and $\pi_L(l) = 1 - \pi_H(l)$ as the probability of the l th time bin in the high state of the Markov chain and that in

the low state of the Markov chain, respectively. Clearly, $\pi_H(l)$ can be expressed as

$$\pi_H(l) = \begin{cases} 1, & \text{if } l = 1 \\ 1 - \alpha, & \text{if } l = 2 \\ (1 - \alpha)^2 + \alpha\beta, & \text{if } l = 3 \\ (1 - \alpha)^3 + 2\alpha\beta(1 - \alpha) + \alpha\beta(1 - \beta), & \text{if } l = 4 \\ \frac{\beta}{\alpha + \beta}, & \text{if } l \geq 5. \end{cases} \quad (15)$$

Note that the steady state probabilities $\pi_H(l)$ and $\pi_L(l)$ are $\pi_H(5) = \beta/(\alpha + \beta)$ and $\pi_L(5) = \alpha/(\alpha + \beta)$.

B. Mean and Variance of the Processed Data for PPM-Based UWB Signals

In the following, we describe the mean and the variance of the processed data z [defined in (12)] for the PPM signal under the UWB channel model described in Section II. Without loss of generality, we take the processed data z_{p1} as an example.

Proposition 1: The average energy of the processed data z_{p1} can be calculated as

$$E[z_{p1}] = \left(\frac{\beta}{\alpha + \beta} \right) \frac{\gamma e^{-3\eta} - \gamma e^{-(L-1)\eta}}{1 - e^{-\eta}} + A \quad (16)$$

where

$$A = 1 + (1 - \alpha)\gamma + [(1 - \alpha)^2 + \alpha\beta] \gamma e^{-\eta} + [(1 - \alpha)^3 + 2\alpha\beta(1 - \alpha) + \alpha\beta(1 - \beta)] \gamma e^{-2\eta}. \quad (17)$$

Proof: See Appendix I. \blacksquare

Proposition 2: The variance of the processed data z_{p1} can be calculated as

$$\begin{aligned} \text{VAR}[z_{p1}] &= 2 \sum_{l=1}^L \sum_{k=1}^{\infty} \frac{1}{k} (E[a_l^2])^2 \left(\frac{\beta}{\alpha + \beta} \frac{\mu_H^k}{k!} e^{-\mu_H} + \frac{\alpha}{\alpha + \beta} \frac{\mu_L^k}{k!} e^{-\mu_L} \right) \\ &+ 2 \sum_{l=1}^{L-1} (\pi_H(5)\pi_H(2) - \pi_H(l)\pi_H(l+1)) E[a_l^2] E[a_{l+1}^2] \\ &+ 2 \sum_{l=1}^{L-2} (\pi_H(5)\pi_H(3) - \pi_H(l)\pi_H(l+2)) E[a_l^2] E[a_{l+2}^2] \\ &+ 2 \sum_{l=1}^{L-3} (\pi_H(5)\pi_H(4) - \pi_H(l)\pi_H(l+3)) E[a_l^2] E[a_{l+3}^2] \\ &+ \sum_{l=1}^{L-\delta} \pi_H(l)\pi_H(\delta+1) E[a_l^2] E[a_{l+\delta}^2] \\ &+ \sum_{l=1}^L \pi_H(l)\sigma_n^2 E[a_l^2] \end{aligned} \quad (18)$$

where $\pi_H(\cdot)$ is defined in (15), $E[a_l^2]$ is described in (5), L is the number of fingers in the RAKE receiver, δ is the modulation index associated with binary PPM, and σ_n is the standard deviation of the Gaussian noise.

Proof: From (12), we can express the variance of the processed data z_{p1} as

$$\begin{aligned} \text{VAR}[z_{p1}] &= \text{VAR}[s_{p1}] + \text{VAR}[r_{p1}] \\ &+ \text{VAR}[n_{p1}] + \text{VAR}[n_{p0}] \\ &+ 2\text{COV}[s_{p1}, r_{p1}] + 2\text{COV}[s_{p1}, n_{p1}] \\ &+ 2\text{COV}[s_{p1}, r_{p0}] + 2\text{COV}[r_{p1}, n_{p1}] \\ &+ 2\text{COV}[r_{p1}, n_{p0}] + 2\text{COV}[n_{p1}, n_{p0}]. \end{aligned} \quad (19)$$

First, we can calculate the signal part $\text{VAR}[s_{p1}]$ as

$$\begin{aligned} \text{VAR}[s_{p1}] &= \text{VAR} \sum_{l=1}^L x_l x_l \\ &= \sum_{l=1}^L \text{VAR}[a_l^2] + 2 \sum_{m=1}^{L-1} \sum_{n=m+1}^L \text{COV}[a_m^2, a_n^2] \\ &= \sum_{l=1}^L \sum_{k=1}^{\infty} \text{VAR}[a_l^2 | n_l = k] \\ &\quad \cdot (\pi_H(l)\text{Prob}[n_l = k, n_{l-1} \neq 0] \\ &\quad + \pi_L(l)\text{Prob}[n_l = k, n_{l-1} = 0]) \\ &\quad + 2 \sum_{l=1}^{L-1} \text{COV}[a_l^2, a_{l+1}^2] + 2 \sum_{l=1}^{L-2} \text{COV}[a_l^2, a_{l+2}^2] \\ &\quad + 2 \sum_{l=1}^{L-3} \text{COV}[a_l^2, a_{l+3}^2]. \end{aligned} \quad (20)$$

Applying the method of [25] to (4) and (15), the first term of (20) can be computed as

$$\begin{aligned} \sum_{l=1}^L \text{VAR}[a_l^2] &= 2 \sum_{l=1}^L \sum_{k=1}^{\infty} \frac{1}{k} (E[a_l^2])^2 \\ &\quad \cdot \left(\pi_H(l) \frac{\mu_H^k}{k!} e^{-\mu_H} + \pi_L(l) \frac{\mu_L^k}{k!} e^{-\mu_L} \right). \end{aligned} \quad (21)$$

From (26), the second term of (20) can be obtained as

$$\begin{aligned} &2 \sum_{l=1}^{L-1} \text{COV}[a_l^2, a_{l+1}^2] \\ &= 2 \sum_{l=1}^{L-1} (E[a_l^2 a_{l+1}^2] - E[a_l^2] E[a_{l+1}^2]) \\ &= 2 \sum_{l=1}^{L-1} ((\pi_H(5)(1 - \alpha)^2 + \pi_L(5)\beta(1 - \alpha)) E[a_l^2] E[a_{l+1}^2] \\ &\quad - \pi_H(l) E[a_l^2] \pi_H(l+1) E[a_{l+1}^2]) \\ &= 2 \sum_{l=1}^{L-1} (\pi_H(5)\pi_H(2) - \pi_H(l)\pi_H(l+1)) E[a_l^2] E[a_{l+1}^2]. \end{aligned} \quad (22)$$

Similarly, we can derive the third and the fourth terms of (20) as

$$\begin{aligned}
& 2 \sum_{l=1}^{L-2} \text{COV} [a_l^2, a_{l+2}^2] \\
&= 2 \sum_{l=1}^{L-2} (\text{E} [a_l^2 a_{l+2}^2] - \text{E} [a_l^2] \text{E} [a_{l+2}^2]) \\
&= 2 \sum_{l=1}^{L-2} ((\pi_H(5)(1-\alpha)^3 + \pi_H(5)(1-\alpha)\alpha\beta \\
&\quad + \pi_L(5)\beta(1-\alpha)^2 + \pi_L(5)\alpha\beta^2) \text{E} [a_l^2] \\
&\quad \cdot \text{E} [a_{l+2}^2] - \pi_H(l)\text{E} [a_l^2] \pi_H(l+2)\text{E} [a_{l+2}^2]) \\
&= 2 \sum_{l=1}^{L-2} (\pi_H(5)\pi_H(3) - \pi_H(l)\pi_H(l+2)) \text{E} [a_l^2] \text{E} [a_{l+2}^2]
\end{aligned} \tag{23}$$

and

$$\begin{aligned}
& 2 \sum_{l=1}^{L-3} \text{COV} [a_l^2, a_{l+3}^2] \\
&= 2 \sum_{l=1}^{L-3} \text{E} [a_l^2] \text{E} [a_{l+3}^2] \\
&\quad \cdot \left\{ \pi_H(5) [(1-\alpha)^4 + (1-\alpha)^2\alpha\beta \right. \\
&\quad \quad + (1-\alpha)\alpha\beta(1-\alpha) + (1-\alpha)\alpha(1-\beta)\beta] \\
&\quad \quad + \pi_L(5) [\beta(1-\alpha)^3 + \beta(1-\alpha)\alpha\beta \\
&\quad \quad \quad \left. + \beta\alpha(1-\beta)\beta + \beta\alpha\beta(1-\alpha)] \right\} \\
&\quad - \pi_H(l)\text{E} [a_l^2] \pi_H(l+3)\text{E} [a_{l+3}^2] \\
&= 2 \sum_{l=1}^{L-3} (\pi_H(5)\pi_H(4) - \pi_H(l)\pi_H(l+3)) \text{E} [a_l^2] \text{E} [a_{l+3}^2].
\end{aligned} \tag{24}$$

From (21)–(24), we can compute $\text{VAR}[s_{p1}]$ of (18). The remaining terms of (18) will be derived in Appendix II. ■

C. SNR for PPM Signal in the UWB Channel

With the mean and the variance of the processed data z , we can compute the energy of a PPM signal in the UWB channel as

$$S_{p1} = \text{E} [s_{p1}^2] = \text{E}[s_{p1}]^2 + \text{VAR}[s_{p1}] \tag{25}$$

where

$$\text{E}[s_{p1}] = \sum_{l=1}^L \pi_H(l)\text{E} [a_l^2]. \tag{26}$$

$\text{E}[a_l^2]$ is given in (5), and $\text{VAR}[s_{p1}]$ can be obtained from (20). As for the noise energy N_{p1} , it can be calculated by

$$\begin{aligned}
N_{p1} &= \text{VAR}[r_{p1}] + \text{VAR}[n_{p1}] + \text{VAR}[n_{p0}] \\
&\quad + \text{E}[r_{p1}]^2 + \text{E}[n_{p1}]^2 + \text{E}[n_{p0}]^2
\end{aligned} \tag{27}$$

where $\text{E}[r_{p1}]$, $\text{E}[n_{p1}]$, $\text{E}[n_{p0}]$, $\text{VAR}[r_{p1}]$, $\text{VAR}[n_{p1}]$, and $\text{VAR}[n_{p0}]$ are given in (50), (51), (52), (53), (55), and (56), respectively. According to the results obtained (25) and (27), we can estimate the SNR_{p1} of the processed data z_{p1} by

$$\text{SNR}_{p1} = \frac{S_{p1}}{N_{p1}}. \tag{28}$$

We will perform simulations to validate the accuracy of the proposed analytical method in Section VI-B.

V. EFFECT OF MULTIPLE TRANSMIT AND RECEIVE ANTENNAS

A. Repetition Codes

Fig. 1(a) shows the scenario of using repetition code with no diversity (Tx1–Rx1) in the case $N_p = 2$. First, we define the processed data $z_{p1.T1}^{(f1)}$ and $z_{p1.T1}^{(f2)}$ in frames 1 and 2 as

$$z_{p1.T1}^{(f1)} = s_{p1.T1} + r_{p1.T1} + n_{p1}^{(f1)} + n_{p0}^{(f1)} \tag{29}$$

and

$$z_{p1.T1}^{(f2)} = s_{p1.T1} + r_{p1.T1} + n_{p1}^{(f2)} + n_{p0}^{(f2)} \tag{30}$$

where s , r , and n represent the signal part, the redundancy part, and the noise part of the processed data z , the superscript (fi) means the i th frame, the subscript $p1$ means the message bit $d^{(i)} = 1$, and the subscript Ti means the i th transmit antenna. Denote the processed data for the no diversity scheme as z_{p1}^{ND} . Then, we have

$$\begin{aligned}
z_{p1}^{\text{ND}} &= z_{p1.T1}^{(f1)} + z_{p1.T1}^{(f2)} \\
&= 2s_{p1.T1} + 2r_{p1.T1} + n_{p1}^{(f1)} + n_{p0}^{(f1)} + n_{p1}^{(f2)} + n_{p0}^{(f2)}.
\end{aligned} \tag{31}$$

From (16), (18), and (31), the mean and variance of the processed data z_{p1}^{ND} can be computed respectively by

$$\begin{aligned}
\text{E} [z_{p1}^{\text{ND}}] &= 2\text{E}[s_{p1.T1}] + 2\text{E}[r_{p1.T1}] \\
&\quad + \text{E} [n_{p1}^{(f1)}] + \text{E} [n_{p0}^{(f1)}] + \text{E} [n_{p1}^{(f2)}] + \text{E} [n_{p0}^{(f2)}]
\end{aligned} \tag{32}$$

and

$$\begin{aligned}
\text{VAR} [z_{p1}^{\text{ND}}] &= \text{VAR}[2s_{p1.T1}] + \text{VAR}[2r_{p1.T1}] + \text{VAR} [n_{p1}^{(f1)}] \\
&\quad + \text{VAR} [n_{p0}^{(f1)}] + \text{VAR} [n_{p1}^{(f2)}] + \text{VAR} [n_{p0}^{(f2)}].
\end{aligned} \tag{33}$$

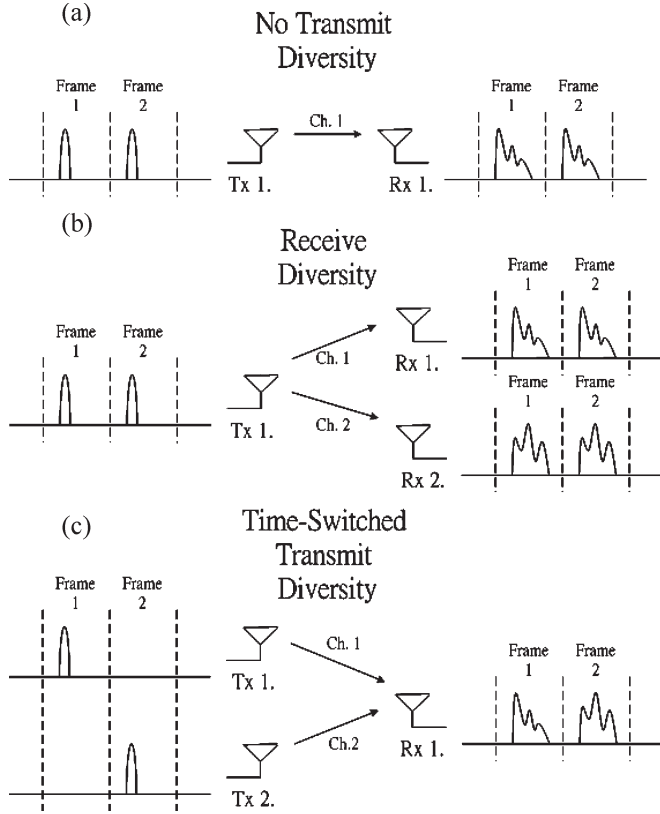


Fig. 1. Diversity schemes. (a) No diversity. (b) Receive diversity. (c) TSTD.

Represent S_{p1}^{ND} and N_{p1}^{ND} as the signal energy and the noise energy of the processed data z_{p1}^{ND} , respectively. Then, we have

$$S_{p1}^{ND} = 4E[s_{p1}]^2 + 4\text{VAR}[s_{p1}] \quad (34)$$

where $\text{VAR}[s_{p1}]$ and $E[s_{p1}]$ can be obtained from (20) and (26), respectively. Furthermore, the noise energy N_{p1}^{ND} can be derived as

$$N_{p1}^{ND} = 2\sigma_n^2 \sum_{l=1}^L \pi_H(l) E[a_l^2] + 2 \sum_{l=1}^{L-\delta} \pi_H(l) \pi_H(1+\delta) E[a_l^2] E[a_{l+\delta}^2]. \quad (35)$$

Thus, by substituting related channel information of a_l and $\pi_H(l)$ into (35), N_{p1}^{ND} can be also obtained analytically. From (34) and (35), we show how to calculate SNR_{p1}^{ND} analytically.

B. Receive Diversity

Consider the receive diversity scheme (Tx1–Rx2) having repetition codes with $N_p = 2$ as shown in Fig. 1(b). We express the processed data z_{p1}^{RD} for the receive diversity scheme as

$$z_{p1}^{RD} = z_{p1.T1}^{ND} + z_{p1.T2}^{ND} \quad (36)$$

where the superscript RD means receive diversity. Clearly, we can use the same method of obtaining $E[z_{p1}^{ND}]$ in (32)

to compute the mean of the processed data z_{p1}^{RD} , which is defined as

$$E[z_{p1}^{RD}] = E[z_{p1.T1}^{ND}] + E[z_{p1.T2}^{ND}]. \quad (37)$$

Likewise, the variance of the processed data z_{p1}^{RD} can be calculated by

$$\text{VAR}[z_{p1}^{RD}] = \text{VAR}[z_{p1.T1}^{ND}] + \text{VAR}[z_{p1.T2}^{ND}]. \quad (38)$$

Denote S_{p1}^{RD} and N_{p1}^{RD} as the signal energy and the noise energy of the processed data z_{p1}^{RD} , respectively, and recall that the (Tx1–Rx2) receive diversity scheme and repetition length $N_p = 2$ is considered. Then, we have

$$S_{p1}^{RD} = 16E[s_{p1}]^2 + 8\text{VAR}[s_{p1}] \quad (39)$$

and

$$N_{p1}^{RD} = 2N_{p1}^{ND}. \quad (40)$$

C. Transmit Diversity

Now, we consider a TSTD (Tx2–Rx1) scheme as shown in Fig. 1(c). For the case with repetition length $N_p = 2$, one can express the processed data z_{p1}^{TD} for the transmit diversity scheme as

$$z_{p1}^{TD} = z_{p1.T1}^{(f1)} + z_{p1.T2}^{(f2)}. \quad (41)$$

Since

$$E[z_{p1}^{TD}] = E[z_{p1.T1}] + E[z_{p1.T2}] = 2E[z_{p1}] \quad (42)$$

we can calculate $E[z_{p1}^{TD}]$ by following the procedures of evaluating $E[z_{p1}]$ in (16). Define ρ as the correlation coefficient between the two transmit antennas. Then, the variance of the processed data z_{p1}^{TD} is

$$\begin{aligned} \text{VAR}[z_{p1}^{TD}] &= \text{VAR}[z_{p1.T1}] + \text{VAR}[z_{p1.T2}] + 2\text{COV}[z_{p1.T1}, z_{p1.T2}] \\ &= 2\text{VAR}[z_{p1}] + 2\rho \left(\sqrt{\text{VAR}[s_{p1.T1}]\text{VAR}[s_{p1.T2}]} \right. \\ &\quad \left. + \sqrt{\text{VAR}[r_{p1.T1}]\text{VAR}[r_{p1.T2}]} \right) \end{aligned} \quad (43)$$

where $\text{VAR}[z_{p1}]$ is defined in (18) of Proposition 2. Thus, we can compute SNR_{p1}^{TD} from

$$S_{p1}^{TD} = 4E[s_{p1}]^2 + 2(1 + \rho)\text{VAR}[s_{p1}] \quad (44)$$

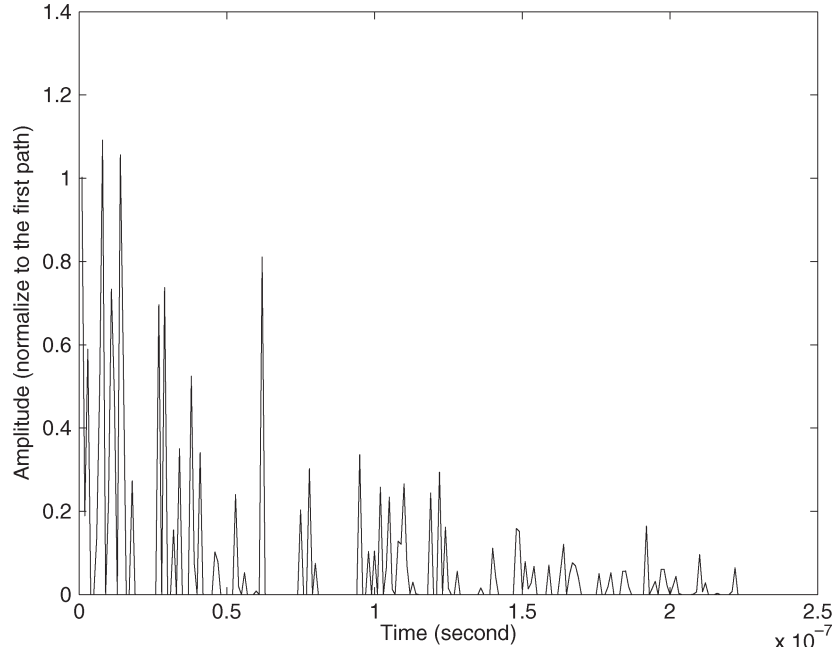


Fig. 2. Example of the UWB channel response in the time domain.

and

$$N_{p1}^{TD} = 2N_{p1}^{ND} \quad (45)$$

where $E[s_{p1}]$, $\text{VAR}[s_{p1}]$, and N_{p1}^{ND} are given in (26), (20), and (35), respectively.

VI. NUMERICAL RESULTS

A. UWB Channel Response

Fig. 2 shows an example of the UWB channel response using the channel model described in Section II, with parameters listed in Table I. In the considered model, the channel response time is set to 225 ns as in [15], the average number of the resolvable paths is 80.72. Let N be the total time bin number during the channel response time, T_A the first path arrival time, and t_l is the arrival time of each resolvable path. Then, in our simulations, the mean excess delay $T_m = (\sum_{l=1}^N (t_l - T_A) a_l^2 / \sum_{l=1}^N a_l^2) = 34.61$ ns, and the root mean square (rms) delay spread $T_{\text{rms}} = ((\sum_{l=1}^N (t_l - T_m - T_A)^2 a_l^2) / (\sum_{l=1}^N a_l^2))^{1/2} = 37.98$ ns.

B. Average SNR and Variance of the Pulse-Based UWB Signals

Fig. 3 compares the SNR of PPM signals for no diversity, receive diversity, and transmit diversity schemes. Through simulations, we validate the analytical results obtained by (34), (35), (39), (40), (44), and (45) in Section IV. In Fig. 3, one can find that the SNR of the receive diversity is the highest, while the no diversity scheme and the transmit diversity have the similar SNR.

TABLE I
SYSTEM PARAMETERS

The UWB pulse width	1 ns
The sampling time (time bin)	1 ns
Simultaneous arrival path number n	A modified Poisson process.
μ_H	2/3
μ_L	1/3
Average resolvable path power	Exponential decay.
γ	-5 dB
β	0.025
The PDF of the received signal power	Gamma distribution.
The diversity schemes	1) no diversity, Tx1-Rx1, 2) receive diversity, Tx1-Rx2, 3) transmit diversity, Tx2-Rx1, 4) transmit diversity, Tx4-Rx1, 5) MIMO, Tx2-Rx2.
The modulation schemes	PPM
The frame number f	2
The RAKE finger number L	10, 30, 50, 100, or 250
The delay time δ associated with PPM	1, 25, 50 ns

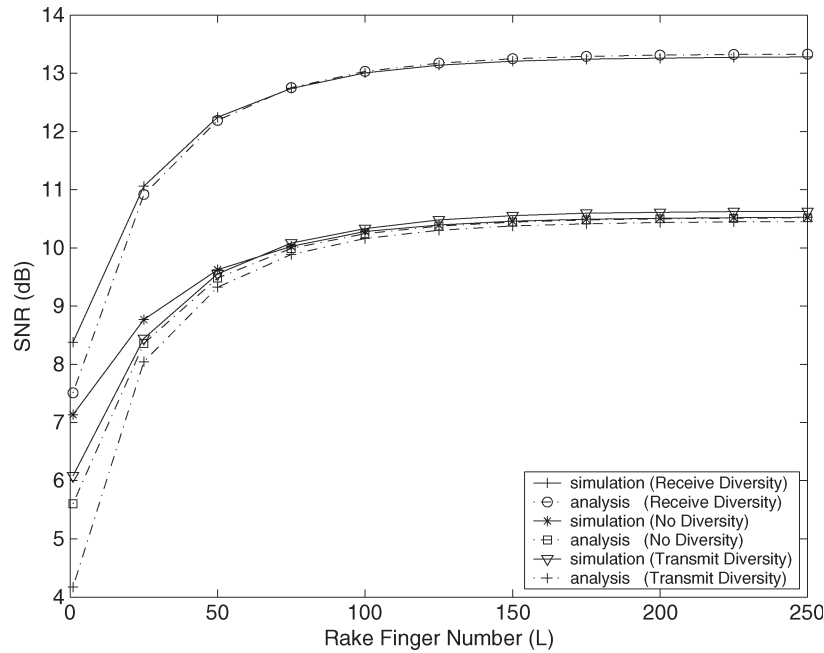


Fig. 3. Analytical and simulation results for the SNR of the PPM signals over the UWB channel with multiple transmit and receive antennas.

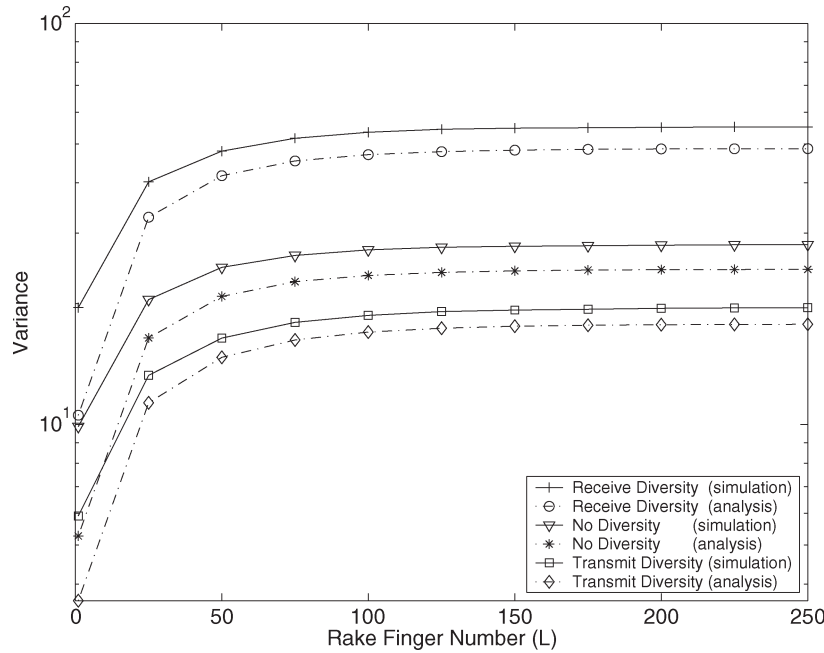


Fig. 4. Analytical and simulation results for the variance of the PPM signals over the UWB channel with multiple transmit and receive antennas.

Fig. 4 shows the variance of PPM signals with no diversity, receive diversity, and transmit diversity schemes in the UWB channel by analysis and simulations. From the viewpoint of the signal variance, transmit diversity is the best, no diversity ranks second, and receive diversity is the worst. Here, we assume that the antennas of both receive diversity and transmit diversity are mutually independent.

Fig. 5 shows the effect of spatial correlation ρ of transmit diversity on the variance of the PPM signals over the UWB channel. As shown in the figure, the variance of the PPM signals increases as the correlation of transmit diversity increases. From the results, it is implied that the diversity gain of transmit

diversity may not be significant in the UWB channel. In the following, we will quantify the performance difference between no diversity and having antenna diversity in terms of BER performance.

C. Comparison for Different Diversity Schemes for the PPM UWB System

Fig. 6 shows the BER performances of different diversity schemes for the binary PPM signals in the UWB channel. In the figure, the numbers adjacent to Tx and Rx represent the numbers of the transmit and receive antennas, L represents the

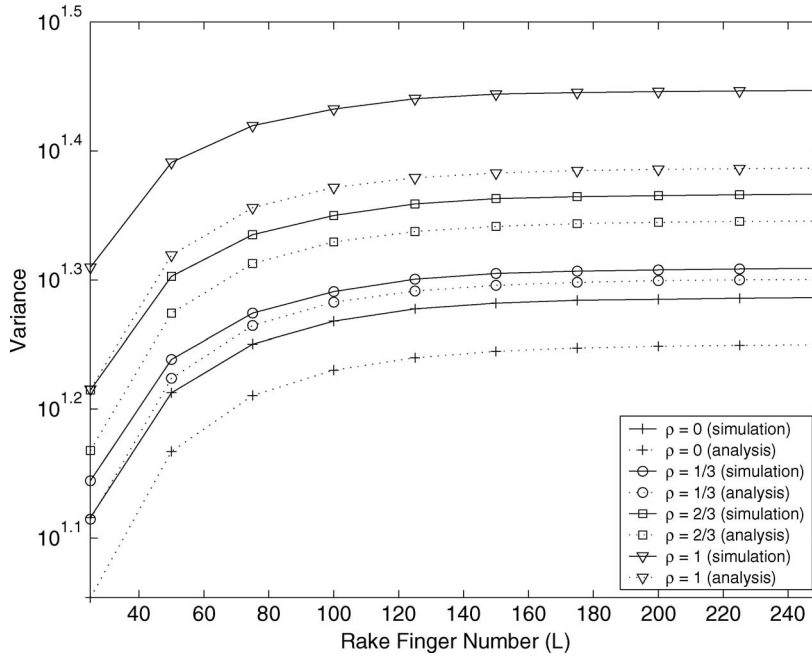


Fig. 5. Effect of spatial correlation of transmit diversity on the variance of the PPM signals over the UWB channel.

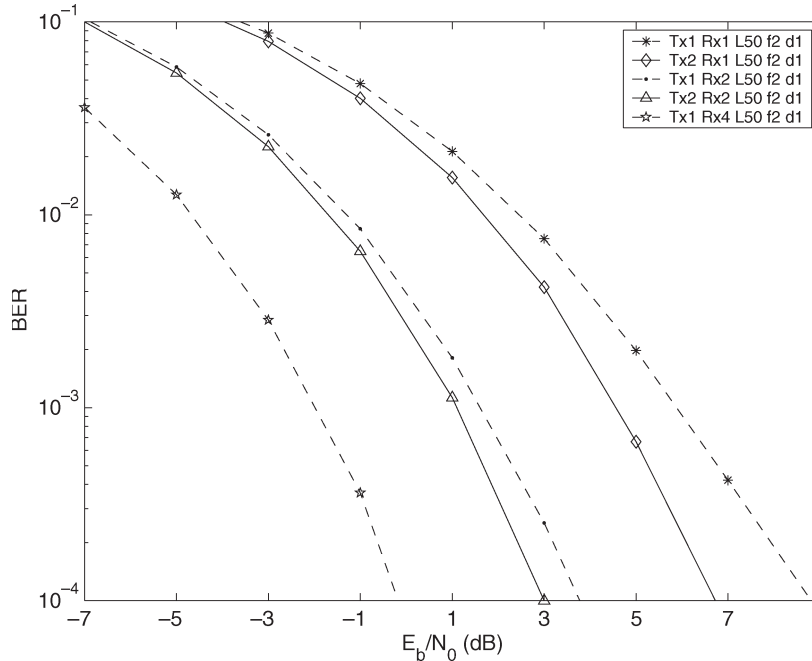


Fig. 6. BER simulation results for the different diversity schemes in the PPM UWB system. Here, Tx and Rx represent the transmit and receive antenna numbers, respectively, L represents the RAKE finger number, f represents the frame number, and δ represents the delay time associated with PPM.

finger number in the RAKE receiver, f represents the frame number, and δ represents the delay time associated with PPM. We derived the two observations from Fig. 6.

- 1) Comparing the no diversity (Tx1–Rx1) scheme to the TSTD (Tx2–Rx1) scheme, one can find that the TSTD scheme can improve BER performance by about 2 dB at $BER = 10^{-4}$. As shown in Fig. 4, the signal of the transmit diversity scheme is more stable than that of the no diversity scheme, which can explain the BER performance improvement of the transmit diversity scheme over

- the no diversity scheme even though the SNRs of these two diversity schemes are about the same in Fig. 3.
- 2) Recall that the diversity order can be roughly viewed as the slope of BER versus SNR in the region with high SNRs where the slope no longer increases. The higher the diversity order, the steeper will be the slope of the performance curve for BER versus SNR. As shown in the figure, the TSTD (Tx2–Rx1) scheme indeed achieves the same diversity order as the receive diversity (Tx1–Rx2) scheme. Furthermore, comparing the Tx2–Rx2 and the Tx1–Rx4 schemes, we find that the

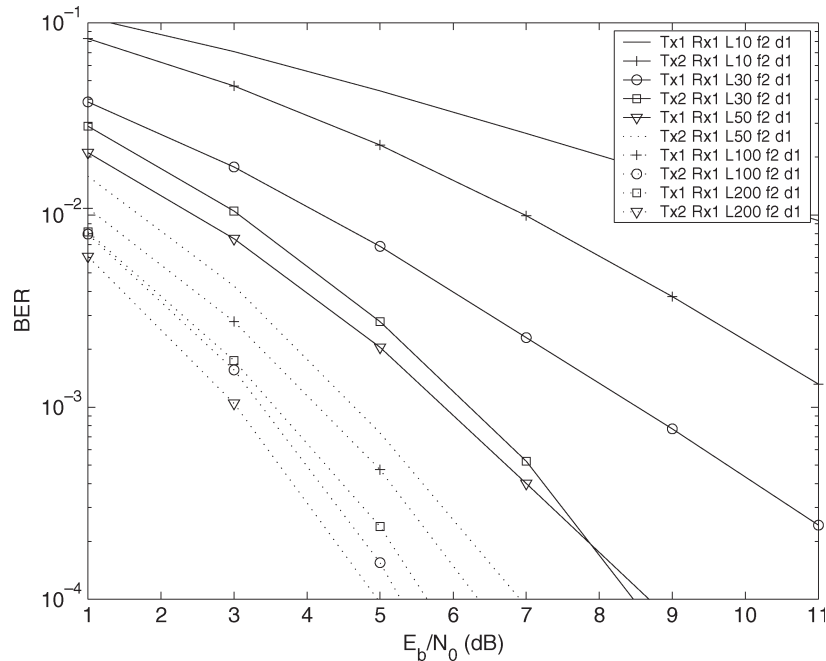


Fig. 7. BER simulations of the PPM UWB system with the different RAKE finger numbers, where Tx and Rx represent the transmit and receive antenna numbers, respectively, L represents the RAKE finger number, f represents the frame number, and δ represents the delay time associated with PPM.

Tx2–Rx2 scheme can achieve about the same diversity order as the Tx1–Rx4 scheme but at the cost of about 3 dB E_b/N_0 loss. In this figure, it is demonstrated that employing multiple TSTD or multiple receive antennas can improve the UWB performance even though the UWB channel possesses inherently rich diversity.

Note that because the MIMO UWB channel may perform differently from the narrowband MIMO channel. For example, severe correlation between channel paths may exist in a UWB channel. Thus, the above results should be used cautiously as an upper bound that quantifies the extent to which transmit or receive antenna combining techniques can improve the performance for the PPM-based UWB system. In the following, we will examine how to exploit transmit diversity in the UWB channel from a different perspective—reducing the complexity of the RAKE receiver.

D. Effect of RAKE Finger Numbers

Fig. 7 shows the BER performance of the PPM UWB system with different RAKE finger numbers. Two major remarks are given as follows.

- 1) The transmit diversity scheme (Tx2–Rx1) with $L = 30$ (with the square legend) has the similar performance to the scheme (Tx1–Rx1) with $L = 50$ (with the triangle legend). It is implied that the complexity of RAKE receiver can be alleviated at the cost of increasing the transmit antennas by using TSTD.
- 2) Because of inherently large path diversity, adding more transmit antennas in the UWB system cannot increase the diversity order significantly. In the figure, the slope

of BER versus SNR for the cases of $L > 50$ with single antenna (with the triangle legend) and that of $L > 30$ with two transmit antennas (with the squared legend) are about the same. Nevertheless, transmit diversity can slightly improve the BER performance for the PPM UWB system from the signal variance perspective as explained in Fig. 4.

VII. CONCLUSION

In this paper, we have derived an analytical expression for the PPM signal in an UWB channel characterized by the cluster effect and highly dense frequency-selective fading. Furthermore, we have demonstrated that the TSTD combined with the template-based pulse detection can improve the performance of the PPM-based UWB system.

Through analysis and simulations, we have the following two major remarks.

- 1) Although multiple transmit or receive antennas cannot deliver diversity gain for the UWB system in the strict sense [i.e., improving the slope of BER versus SNR], multiple transmit antennas can improve the system performance in the manner of reducing signal variations. Thus, transmit antennas can be used to reduce receiver complexity since the number of fingers of a RAKE receiver in the UWB system can be very high.
- 2) Multiple receive antennas can provide higher antenna array combining gain. Because the transmitted power in the UWB system is extremely low, multiple receive antennas techniques can be an effective approach to improve the performance from the view point of coverage extension.

Some possible interesting research topics that can be extended from this work include the derivation of analytical BER performance for the PPM signals in the highly dense frequency-selective fading channel. Furthermore, it is worth developing an analytical model to incorporate the effect of time-hopping and multiple access interference in a MIMO UWB system with clustering property and highly dense frequency-selective fading. Last but not the least, the provided analytical method to calculate the signal energy in the UWB channel can be extended to the PAM case.

APPENDIX I PROOF OF PROPOSITION 1

From (2) and (12), we can express the mean of the processed data z_{p1} as

$$E[z_{p1}] = E[s_{p1}] + E[r_{p1}] + E[n_{p1}] + E[n_{p0}] \quad (46)$$

where the signal part $E[s_{p1}]$ is defined as

$$E[s_{p1}] = E \left[\sum_{l=1}^L x_l x_l \right] = \sum_{l=1}^L E [\xi_l^2]. \quad (47)$$

From (5) and (15), we can have

$$\sum_{l=1}^L E [\xi_l^2] = A + B \quad (48)$$

where A is defined in (17) and

$$\begin{aligned} B &= \sum_{l=5}^L (\pi_H(1 - \alpha) + \pi_L\beta) E [a_l^2] \\ &= \sum_{l=5}^L \left(\frac{\beta}{\alpha + \beta}(1 - \alpha) + \frac{\alpha}{\alpha + \beta}\beta \right) E [a_l^2] \\ &= \left(\frac{\beta}{\alpha + \beta} \right) \frac{\gamma e^{-3\eta} - \gamma e^{-(L-1)\eta}}{1 - e^{-\eta}}. \end{aligned} \quad (49)$$

Recalling that b_l in (2) is ± 1 equiprobable, we can calculate the redundancy part $E[r_{p1}]$ of the processed data mean $E[z_{p1}]$ from (12) as

$$\begin{aligned} E[r_{p1}] &= -E \left[\sum_{l=1}^{L-\delta} x_l x_{l+\delta} \right] \\ &= -E \left[\sum_{l=1}^{L-\delta} a_l b_l a_{l+\delta} b_{l+\delta} \right] \\ &= -\sum_{l=1}^{L-\delta} E[a_l a_{l+\delta}] E[(b_l b_{l+\delta})] \\ &= 0. \end{aligned} \quad (50)$$

Note that n_l is a Gaussian random variable with zero mean, and x_l and n_l are mutually independent. Thus, from (12), we

can express the \mathbf{p}_1 noise part $E[n_{p1}]$ of the processed data mean $E[z_{p1}]$ as

$$E[n_{p1}] = E \left[\sum_{l=1}^L n_{l+\delta} x_l \right] = \sum_{l=1}^L E[n_{l+\delta}] E[x_l] = 0. \quad (51)$$

Similar to (51), the \mathbf{p}_0 noise part $E[n_{p0}]$ of the processed data mean $E[z_{p1}]$ can be calculated as

$$E[n_{p0}] = E \left[\sum_{l=1}^L n_l x_l \right] = \sum_{l=1}^L E[n_l] E[x_l] = 0. \quad (52)$$

Form (46), we prove Proposition 1.

APPENDIX II PROOF OF PROPOSITION 2

In this appendix, we derive the remaining terms of the right-hand side of (18) except $\text{VAR}[s_{p1}]$. For the redundancy part $\text{VAR}[r_{p1}]$ of the processed data, we first consider the ideal pulse in the worst case of $\delta = 1$. Since b_l is equiprobable to take on the value ± 1 , it is obvious that $E[b_l] = 0$. Recalling (2), (8), and (12), we can obtain

$$\begin{aligned} \text{VAR}[r_{p1}] &= \text{VAR} \left[-\sum_{l=1}^{L-1} x_l x_{l+1} \right] \\ &= \text{VAR} \left[-\sum_{l=1}^{L-1} \xi_l \xi_{l+1} \right] \\ &= \sum_{l=1}^{L-1} \text{VAR}[a_l b_l a_{l+1} b_{l+1}] \\ &\quad + 2 \sum_{m=1}^{L-1} \sum_{n=m+1}^{L-1} \text{COV}[a_m b_m a_{m+1} b_{m+1}, a_n b_n a_{n+1} b_{n+1}] \\ &= \sum_{l=1}^{L-1} \text{VAR}[a_l b_l a_{l+1} b_{l+1}] \\ &= \sum_{l=1}^{L-1} E [a_l^2 a_{l+1}^2 b_l^2 b_{l+1}^2] - E[a_l a_{l+1} b_l b_{l+1}]^2 \\ &= \sum_{l=1}^{L-1} E [a_l^2 a_{l+1}^2] E [b_l^2 b_{l+1}^2] \\ &= \sum_{l=1}^{L-1} \pi_H(l) \pi_H(2) E [a_l^2] E [a_{l+1}^2]. \end{aligned} \quad (53)$$

For the more general case $\delta \neq 1$, one can derive

$$\text{VAR}[r_{p1}] = \sum_{l=1}^{L-\delta} \pi_H(l) \pi_H(\delta+1) \text{E}[a_l^2] \text{E}[a_{l+\delta}^2]. \quad (54)$$

Next, we derive the noise part $\text{VAR}[n_{p1}]$ of the processed data variance $\text{VAR}[z_{p1}]$. For the Gaussian noise with zero mean and the variance of $\sigma_n^2/2$

$$\begin{aligned} \text{VAR}[n_{p1}] &= \text{VAR} \left[\sum_{l=1}^L n_{l+1} x_l \right] \\ &= \sum_{l=1}^L \text{VAR}[n_{l+1} x_l] \\ &\quad + 2 \sum_{m=1}^{L-1} \sum_{n=m+1}^L \text{COV}[n_{m+1} x_m, n_{n+1} x_n] \\ &= \sum_{l=1}^L \frac{\pi_H(l) \sigma_n^2}{2} \text{E}[a_l^2]. \end{aligned} \quad (55)$$

Similarly, we can obtain

$$\text{VAR}[n_{p0}] = \sum_{l=1}^L \frac{\pi_H(l) \sigma_n^2}{2} \text{E}[a_l^2] \quad (56)$$

and

$$\begin{aligned} \text{COV}[s_{p1}, r_{p1}] &= \text{E}[s_1 r_{p1}] - \text{E}[s_1] \text{E}[r_1] \\ &= \sum_{l=1}^{L-1} \pi_H(l) \pi_H(2) \text{E}[a_l | n_l \neq 0] \text{E}[a_l^2] \text{E}[a_{l+1}^2] \\ &= 0. \end{aligned} \quad (57)$$

Last, it is easy to show that

$$\begin{aligned} \text{COV}[s_{p1}, r_{p1}] &= \text{COV}[s_{p1}, n_{p1}] = \text{COV}[s_{p1}, n_{p0}] \\ &= \text{COV}[r_{p1}, n_{p1}] = \text{COV}[r_{p1}, n_{p0}] \\ &= \text{COV}[n_{p1}, n_{p0}] = 0. \end{aligned} \quad (58)$$

Hence, from (21)–(24) and (53)–(58), we have proven Proposition 2.

ACKNOWLEDGMENT

The authors are thankful for the valuable comments by Prof. A. Svensson and anonymous reviewers. The authors thank Prof. M. Z. Win and A. F. Molisch for their UWB tutorial course and helpful discussions.

REFERENCES

[1] K. Siwiak and D. McKeown, *Ultra-Wideband Radio Technology*. Chichester, U.K.: Wiley, 2004, pp. 39–52.

[2] K. Siwiak, “Ultra-wide band radio: Introducing a new technology,” in *IEEE Vehicular Technology Conf.*, Rhodes, Greece, Spring 2001, vol. 2, pp. 1088–1093.

[3] M. Z. Win and R. A. Scholtz, “Impulse radio: How it works,” *IEEE Commun. Lett.*, vol. 2, no. 2, pp. 36–38, Feb. 1998.

[4] —, “Ultra-wide bandwidth time-hopping spread-spectrum impulse radio for wireless multiple-access communications,” *IEEE Trans. Commun.*, vol. 48, no. 4, pp. 679–689, Apr. 2000.

[5] —, “Characterization of ultra-wide bandwidth wireless indoor channels: A communication-theoretic view,” *IEEE J. Sel. Areas Commun.*, vol. 20, no. 9, pp. 1613–1627, Dec. 2002.

[6] S. M. Alamouti, “A simple transmit diversity technique for wireless communications,” *IEEE J. Sel. Areas Commun.*, vol. 16, no. 8, pp. 1451–1458, Oct. 1998.

[7] V. Tarokh, H. Jafarkhani, and A. R. Calderbank, “Space–time block codes from orthogonal designs,” *IEEE Trans. Inf. Theory*, vol. 45, no. 5, pp. 1456–1467, Jul. 1999.

[8] V. Tarokh, N. Seshadri, and A. R. Calderbank, “Space–time codes for high data rate wireless communication: Performance criterion and code construction,” *IEEE Trans. Inf. Theory*, vol. 44, no. 2, pp. 744–765, Mar. 1998.

[9] A. F. Naguib, V. Tarokh, N. Seshadri, and A. R. Calderbank, “A space–time coding modem for high-data-rate wireless communications,” *IEEE J. Sel. Areas Commun.*, vol. 16, no. 8, pp. 1459–1478, Oct. 1998.

[10] H. E. Gamal, A. R. Hammons, Y. Liu, M. P. Fitz, and O. Y. Takeshita, “On the design of space–time and space–frequency codes for MIMO frequency-selective fading channels,” *IEEE Trans. Inf. Theory*, vol. 49, no. 9, pp. 2277–2292, Sep. 2003.

[11] A. Sibille and S. Bories, “Spatial diversity for UWB communications,” in *5th Eur. Personal Mobile Communications Conf. (EPMCC)*, Glasgow, U. K., Apr. 2003, pp. 367–370.

[12] S. S. Tan, B. Kannan, and A. Nallanathan, “Ultra-wideband impulse radio systems with temporal and spatial diversities,” in *IEEE Vehicular Technology Conf., Fall*, Orlando, FL, Oct. 2003, pp. 607–611.

[13] M. Weisenhorn and W. Hirt, “Performance of binary antipodal signaling over the indoor UWB MIMO channel,” in *IEEE Int. Conf. Communications*, Anchorage, AK, May 2003, pp. 2872–2878.

[14] L. Yang and G. B. Giannakis, “Analog space–time coding for multi-antenna ultra-wideband transmissions,” *IEEE Trans. Commun.*, vol. 52, no. 3, pp. 507–517, Mar. 2004.

[15] F. Zhu, Z. Wu, and C. R. Nassar, “Generalized fading channel model with application to UWB,” in *IEEE Conf. Ultra Wideband Systems and Technologies*, Baltimore, MD, 2002, pp. 13–17.

[16] H. Hashemi, “Impulse response modeling of indoor radio propagation channels,” *IEEE J. Sel. Areas Commun.*, vol. 11, no. 7, pp. 967–978, Sep. 1993.

[17] M. Z. Win, F. Ramirez-Mireles, R. A. Scholtz, and M. A. Barnes, “Ultra-wide bandwidth (UWB) signal propagation for outdoor wireless communications,” in *IEEE Vehicular Technology Conf.*, Phoenix, AZ, May 1997, vol. 1, pp. 251–255.

[18] M. Z. Win, R. A. Scholtz, and M. A. Barnes, “Ultra-wide bandwidth signal propagation for indoor wireless communications,” in *IEEE Int. Conf. Communications*, Montreal, QC, Canada, Jun. 1997, vol. 1, pp. 56–60.

[19] D. Cassioli, M. Z. Win, and A. F. Molisch, “A statistical model for the UWB indoor channel,” in *IEEE Vehicular Technology Conf., Spring*, Rhodes, Greece, 2001, vol. 2, pp. 1159–1163.

[20] J. Keignart and N. Daniele, “Subnanosecond UWB channel sounding in frequency and temporal domain,” in *IEEE Conf. Ultra Wideband Systems and Technologies*, Baltimore, MD, 2002, pp. 25–30.

[21] J. Foerster *et al.*, “Channel modeling sub-committee report final,” IEEE P802.15 Wireless Personal Area Networks, VOCAL Technologies, Ltd., Amherst, NY, P802.15-02/490r1-SG3a, Feb. 2003.

[22] R. T. Derryberry, S. D. Gray, D. M. Ionescu, G. Mandyam, and B. Raghathan, “Transmit diversity in 3G CDMA systems,” *IEEE Commun. Mag.*, vol. 40, no. 4, pp. 68–75, Apr. 2002.

[23] R. C. Qiu, “A generalized time domain multipath channel and its application in ultra-wideband (GWU) wireless optimal receiver design: System performance analysis,” in *IEEE Wireless Communication and Network Conf.*, Atlanta, GA, Mar. 2004, pp. 901–907.

[24] A. Leon-Garcia, *Probability and Random Processes for Electrical Engineering*, 2nd ed. Reading, MA: Addison-Wesley, 1994, p. 466.

[25] H. Stark and J. W. Woods, *Probability and Random Processes With Application to Signal Processing*, 3rd ed. Englewood Cliffs, NJ: Prentice-Hall, 2002, pp. 322–323.



Li-Chun Wang (S'92–M'96) received the B.S. degree in electrical engineering from the National Chiao-Tung University (NCTU), Hsinchu, Taiwan, R.O.C., in 1986, the M.S. degree in electrical engineering from the National Taiwan University, Taipei, in 1988, and the M.S. and Ph.D. degrees in electrical engineering from the Georgia Institute of Technology, Atlanta, in 1995 and 1996, respectively.

From 1990 to 1992, he was with the Telecommunications Laboratories of the Ministry of Transportations and Communications, Taiwan (currently the Telecom Labs of Chunghwa Telecom Co.). In 1995, he was affiliated with Bell Northern Research of Northern Telecom, Inc., Richardson, TX. From 1996 to 2000, he was with AT&T Laboratories, where he was a Senior Technical Staff Member in the Wireless Communications Research Department. Since August 2000, he has been an Associate Professor in the Department of Communication Engineering of the NCTU. He holds three U.S. patents and one more pending. His current research interests are in the areas of cellular architectures, radio network resource management, and cross-layer optimization for high-speed wireless networks.

Dr. Wang was a co-recipient of the Jack Neubauer Memorial Award in 1997, which recognizes the best systems paper published in the IEEE TRANSACTIONS ON VEHICULAR TECHNOLOGY. Currently, he is the Editor of the IEEE TRANSACTIONS ON WIRELESS COMMUNICATIONS.



Wei-Cheng Liu (S'04) received the B.S. and M.S. degrees from the National Tsing Hua University, Hsinchu, Taiwan, R.O.C., in 1999 and 2001, respectively, both in electrical engineering. He is currently working toward the Ph.D. degree in communication engineering at the Department of Communication Engineering, National Chiao-Tung University, Hsinchu.

After he earned the M.S. degree, he served the military in Cheng Gong Ling, Taichung, Taiwan, R.O.C. In 2002, he was a GSM Layer 1 Software Engineer at Compal Communications, Inc., Taipei, Taiwan. His current research interests are in the areas of cross-layer rate adaptation for wireless local area networks (LANs), ultrawideband (UWB), and multiple-input multiple-output orthogonal frequency division multiplexing (MIMO-OFDM) systems.

Kuan-Jiin Shieh was born in Taiwan, R.O.C., in 1978. He received the B.S. and M.S. degrees in communication engineering from the Department of Communication Engineering, National Chiao-Tung University, Hsinchu, Taiwan.